sides and in films produced from both the poly(amide ester) and the poly(amide acid). Again we attribute the formation of these layers to the greater thermal stability of H_3FeCl_6. Although we found that $FeCl_3$ was formed in the bulk of the film, we feel this can partition into the imidizing film during the thermal process ($FeCl_3$ mp = 306 °C) and migrate to the air- and glass-side surfaces. In the case of the poly(amide acid) the $FeCl_3$ may initiate its migration after imidization has occurred, while in the case of the poly(amide ester) no acid coordination sites exist; therefore, migration most likely occurred throughout the curing process. These postulates are consistent with the surface layers observed via TEM. The poly(amide ester)-derived modified films contained larger surface layers as compared to the poly(amide acid)-derived films.

In summary, we find that both the thermal stability of the dopant and the presence of coordination sites on the polyimide precursor affect the formation of large bulk particles and surface layers. It was observed that the thermal stability of the dopant material made a large contribution to the migration process. However, the percent conversion to a magnetic iron oxide of the metal dopant had to be sacrificed in order to obtain the enhanced migration (5% versus 95% conversion for the H_3FeCl_6 and $Fe(acac)_3$ modified films respectively).

Acknowledgment. We thank Allco Chemical Co. for providing the BTDA and PMDA. We also thank Harshaw Chemical Co. for providing the $Fe(acac)_3$. We gratefully acknowledge financial assistance from the National Aeronautics and Space Administration at Langley Research Center. We also thank Dr. James Rancourt for helpful discussions and Mr. James Hollenhead for his assistance in obtaining TEMs.

Structural Investigations of New Calcium–Rare Earth (R) Oxyborates with the Composition $Ca_4RO(BO_3)_3$

R. Norrestam* and M. Nygren

Departments of Inorganic and Structural Chemistry, Arrhenius Laboratory, Stockholm University, S-10691 Stockholm, Sweden

J.-O. Bovin

National Center for HREM, Chemical Center, University of Lund, P.O. Box 124, S-22100 Lund, Sweden

Received March 5, 1991. Revised Manuscript Received February 13, 1992

A new series of calcium containing rare earth (R) borates has been synthesized by high-temperature synthesis for some of the trivalent R ions, viz., La^{3+}, Nd^{3+}, Sm^{3+}, Gd^{3+}, Er^{3+}, and Y^{3+}. Characterization by X-ray diffraction and electron microscopy techniques has shown them to be isostructural with the compositions $Ca_4RO(BO_3)_3$. The structure type of these new oxyborates, determined by single-crystal X-ray diffraction methods applied to the Sm compound, is related to the structure of a recently found calcium fluoroborate and also to common fluorapatite. For $Ca_4SmO(BO_3)_3$ the unit cell parameters are a = 8.114 (2), b = 16.061 (4), c = 3.579 (1) Å and β = 101.38 (3)°. The space group is monoclinic noncentrosymmetric Cm with Z = 2. The structural model deduced was refined versus the amplitudes of the 547 most significant X-ray reflections, with $\sin(\theta)/\lambda \leq 0.65$ Å^{-1}, to an R value of 0.016. The occurrence of Ca, Sm, O, and B in the synthesized crystals were verified by parallel recording of electron energy-loss spectra (PEELS) in a high-resolution transmission electron microscope (HRTEM). The composition of the crystal used for the X-ray structure investigation was determined by energy-dispersive X-ray analysis (EDX) analysis in a scanning electron microscope to be $Ca_{3.90}Sm_{1.10}O(BO_3)_3$. Studies on analogues of the present compounds toward their possible applications as a high-Nd concentration minilaser materials are in progress.

Introduction

For smaller trivalent ions, like those in the first row, a series of borates known as the pinakiolite family are frequently formed with divalent ions. The composition of this family is $(M^{2+})_2M^{3+}O_2BO_3$ and the structure type is formed for a large variety of divalent and trivalent ions (cf. Norrestam and Bovin[1]). In attempts to synthesize pinakiolite-related phases containing Ca^{2+} and trivalent rare earth ions (including Y^{3+}), it soon became apparent that some unknown phases occurred. X-ray powder diagrams indicated that the phases obtained were mostly isostructural. Preliminary studies of their energy-dispersive X-ray spectra collected in a scanning electron microscope suggested a composition of $Ca_4RO(BO_3)_3$, indicating that a new oxyborate type had been found. To characterize these new phases, crystalline specimens were prepared, and the present structural study of the Sm compound was carried out.

The number of well-characterized solid alkaline earth–rare earth borates is so far very small and includes the Sr^{2+}-containing phase $Sr_3R_2(BO_3)_4$ (see, e.g., Abdullaev and Mamedov[2]) and the Ba^{2+}-containing phase[3] with similar composition, $Ba_3R_2(BO_3)_4$, but with a different structure. Recently another family of oxyborates, with the composition $A_6MM'(BO_3)_6$ where A = Sr or Ba, has been found.[4,5] The metal ions M and M′ comprise several metal ions,

(1) Norrestam, R.; Bovin, J.-O. *Z. Kristallogr.* **1987**, *181*, 135.

(2) Abdullaev, G. K.; Mamedov, K. S. *Kristallografiya* **1982**, *27*, 795.
(3) Yan, J. F.; Hong, H. Y.-P. *Mater. Res. Bull.* **1987**, *22*, 1347.
(4) Thompson, P. D.; Keszler, D. A. *Chem. Mater.* **1989**, *1*, 292.
(5) Schaffers, K. I.; Alekel, III, T.; Thompson, P. D.; Cox, J. R.; Keszler, D. A. *Chem. Mater.* **1989**, *1*, 7068.

0897-4756/92/2804-0737$03.00/0

Table I. Experimental Conditions for the Crystal Structure Determination of Calcium Samarium Oxyborate, $Ca_4SmO(BO_3)_3$

formula weight	503.1
space group	*Cm*
unit cell dimensions	a = 8.114 (2), b = 16.061 (4), c = 3.579 (1) Å, β = 101.38 (3)°
unit cell volume, V	457.2 (2) Å^3
formula units per unit cell, Z	2
calculated density, D_x	3.654 (2) g cm^{-3}
radiation	Mo Kα
wavelength	0.710 69 Å
temperature, T	291 (1) K
crystal shape	needle
crystal size	0.034 × 0.034 × 0.18 mm
diffractometer	Siemens/Stoe AED 2
determination of unit cell	least squares
no. of reflections used	28
θ range	9.1–15.3°
intensity data collection	$\omega/2\theta$ scan technique
maximum $\sin(\theta)/\lambda$	0.65 Å^{-1}
range of h, k, and l	−10 to 10, 0 to 20, and 0 to 4
standard reflections	(0 10 0), (1 4 0), and (−2 6 2)
intensity instability	<1%
no. of observed reflns	676
no. of unique reflns	552
no. of significant reflns	547 (i.e., 99%)
criterion for significance	$I > 5\sigma(I)$
internal R_{int} value	0.024
absorption correction	numerical integration
linear absorbtion coefficient	86.8 cm^{-1}
transmission factor range	0.72–0.78
structure determination technique	heavy atom methods
structure refinement:	full matrix least-squares
minimization of	$\sum w(\Delta F)^2$
anisotropic thermal model for	all atom types but B
number of refined parameters	78
weighting scheme	$(\sigma(R)^2 + 0.0001\|F\|^2)^{-1}$
final R	0.016
final wR	0.020
final max Δ/σ	<0.001
final max and min of $\Delta\rho$	1.1 and −1.4 e$^-$ Å^{-3}

whose sums of formal charges add up to +6. In general, rare earth borates containing, among others, Nd could be of greater importance as they might be potential miniature laser materials.[3]

Experimental Section

Specimens of the calcium–rare earth (R) compounds, $Ca_4RO(BO_3)_3$, were prepared by simply heating a stoichiometric mixtures of $CaCO_3$, R_2O_3, and B_2O_3 at 1100 °C in an open platinum crucible in air. To show the general tendency of trivalent rare earth ions to adopt this structure, specimens were prepared for R = La^{3+} Nd^{3+}, Sm^{3+}, Gd^{3+}, Er^{3+}, and Y^{3+}. The specimens were studied by differential thermal analysis (DTA). The DTA thermograms showed that all compounds melted congruently.

For the $Ca_4SmO(BO_3)_2$ compound that was selected for the X-ray single-crystal diffraction studies, small prismatic crystals were obtained by heating for a few days and then allowing the furnace to cool down to room temperature within 5 h.

X-ray Diffraction Studies. X-ray diffraction photographs, using de Jong and precession techniques, for a selected crystal of $Ca_4SmO(BO_3)_3$, indicated monoclinic symmetry and the possible space groups *C*2, *Cm*, and *C*2/*m*.

The single-crystal X-ray diffraction data, collected with a single-crystal diffractometer, were corrected for background, Lorentz, polarization, and absorption effects. To ensure the validity of the numerical absorption correction (Gaussian integration over the crystal volume) and of the description of the crystal, the effects on a small X-ray data set consisting of 160 intensities collected at various ψ ($\Delta\psi \approx 10°$) for five different reflections (for which the intensity variations were significant) were checked and found to give a statistically significant decrease in internal R value (from 0.059 to 0.046) for the intensities of each reflection. Further relevant experimental conditions are listed in Table I.

Initial metal atom coordinates were derived from a calculated Patterson map and those of the oxygen and boron atoms from subsequent difference electron density ($\Delta\rho$) maps. A reasonable interpretation of the Patterson map could be derived only by assuming that the Sm atoms occupied one special 2-fold position (x,0,z) and the Ca atoms two general 4-fold positions of the noncentrosymmetric spacegroup *Cm*. Thus, the origin along the polar x and z axis of the space group could be defined by keeping the x and z parameters of the Sm atom fixed to zero. A noncentrosymmetric space group symmetry is indicated by the intensity statistics derived from the observed normalized structure factor amplitudes. Thus, the observed average of, e.g., $|E|$ is 0.93. The corresponding theoretical value for a noncentrosymmetric electron density distribution is 0.886 and for the centrosymmetric case 0.798. The presence of a substantial amount of electron density at the origin of the unit cell, as in the present case with Sm at this position, will systematically affect the intensity distributions and to some extent limit the relevance of the derived statistics. Typically the expected effect will be that, i.e., the fraction of small (<0.5) and high (>1.5) estimated $|E|$ values are decreased. The estimated fraction of $|E|$ values below 0.5 is only 11% and the fraction above 1.5 only 4%. The theoretical values for noncentrosymmetric/centrosymmetric distributions are 22.1/38.3% for $|E| < 0.5$ and 10.5/13.4% for $|E| > 1.5$.

The choice of the noncentrosymmetric space group *Cm* is fully supported by the outcome of the structural refinements. Refining the structural model, allowing all but the boron ions to vibrate anisotropically (78 parameters and 550 observations) and without including the imaginary parts of the anomalous dispersion corrections to the atomic scattering factors, gave a weighted wR value of 0.025. When including dispersion corrections to the scattering factors the wR values became 0.020 and 0.037, respectively, for the two possible alternative absolute structure models (one with the y coordinates inverted). The drop in the wR value for the best absolute structure model, when including dispersion correction, corresponds to a wR ratio of 1.25 or an α value less than 10^{-12}. From a statistical point of view[6] this shows that the effects of dispersion correction are significant (further supporting also the choice of a noncentrosymmetric symmetry) and that the correct absolute structure can be selected from the X ray data.

The final atomic coordinates and thermal parameters are given in Table II. The most relevant interatomic distances are listed in Table III. The structural refinements were performed by means of the SHELX-76 program package,[7] using atomic X-ray

Table II. Fractional Atomic Coordinates (×10^4) and Thermal Parameters (×10^4 Å^2) for the Structure of $Ca_4SmO(BO_3)_3$[a]

atom	x	y	z	U_{eq}
Sm	0	0	0	76 (1)
Ca(1)	3579 (1)	1130 (1)	−3295 (3)	49 (3)
Ca(2)	2357 (1)	3184 (1)	3431 (3)	96 (3)
O(1)	1734 (9)	0	5796 (22)	72 (17)
O(2)	4099 (5)	3560 (3)	−816 (11)	112 (11)
O(3)	308 (6)	2690 (3)	−2790 (12)	143 (11)
O(4)	2049 (5)	1711 (3)	1125 (11)	127 (11)
O(5)	364 (5)	4255 (2)	2490 (12)	114 (11)
O(6)	−2042 (9)	0	3928 (22)	120 (20)
B(1)	−3787 (11)	0	2957 (24)	63 (14)
B(2)	481 (8)	1947 (4)	−838 (17)	66 (10)

atom	U_{11}	U_{22}	U_{33}	U_{23}	U_{13}	U_{12}
Sm	54 (2)	119 (2)	53 (2)	0	23 (1)	0
Ca(1)	38 (5)	55 (5)	49 (4)	−1 (4)	10 (4)	−6 (4)
Ca(2)	78 (5)	127 (5)	77 (5)	−10 (4)	31 (4)	−6 (4)
O(1)	37 (27)	69 (28)	105 (31)	0	23 (23)	0
O(2)	63 (19)	119 (18)	144 (20)	8 (16)	58 (15)	29 (16)
O(3)	167 (20)	115 (18)	134 (19)	53 (16)	76 (16)	40 (16)
O(4)	102 (20)	157 (19)	114 (18)	22 (16)	32 (16)	50 (16)
O(5)	120 (20)	89 (18)	124 (19)	−11 (16)	27 (16)	−40 (16)
O(6)	23 (29)	236 (38)	97 (33)	0	−4 (24)	0

[a] The equivalent isotropic thermal parameters (U_{eq}) for the Sm, Ca and O atoms were estimated as $^1/_3$ trace (U). The anisotropic temperature factor expression used for the Sm, Ca and O atoms is $\exp[-2\pi^2((ha^*)^2U_{11} + ... + 2hka^*b^*U_{12})]$.

(6) Rogers, D. *Acta Crystallogr.* 1981, *A37*, 734.

Table III. Metal–Oxygen Bond Distances (Å) in the Coordination Polyhedra of the $Ca_4SmO(BO_3)_3$ Structure

atoms	distance	atoms	distance
Sm–O(1)	2.254 (7)	Ca(2)–O(2)	2.350 (5)
–O(1)	2.265 (7)	–O(2)	2.335 (5)
–O(2)	2.426 (5)	–O(3)	2.625 (5)
–O(2)	2.426 (5)	–O(3)	2.472 (5)
–O(6)	2.459 (7)	–O(3)	2.873 (5)
–O(6)	2.375 (7)	–O(4)	2.502 (5)
–O(4)	3.196 (5)	–O(5)	2.339 (5)
–O(4)	3.196 (5)	–O(6)	2.957 (7)
Ca(1)–O(1)	2.334 (7)	B(1)–O(5)	1.374 (9)
–O(3)	2.344 (5)	–O(5)	1.374 (9)
–O(4)	2.329 (5)	–O(6)	1.390 (9)
–O(4)	2.385 (5)		
–O(5)	2.370 (5)	B(2)–O(2)	1.387 (8)
–O(5)	2.363 (5)	–O(3)	1.376 (8)
		–O(4)	1.380 (8)

scattering factors for neutral atoms from the *International Tables for Crystallography*.[8] The structural diagrams were obtained with the graphics program ATOMS.[9]

From the collected single-crystal intensity data for $Ca_4SmO(BO_3)_3$, the expected X-ray powder photograph was calculated. With this result the powder photographs obtained with a Guinier camera, using Cu Kα radiation and with silicon as internal standard, can easily be interpreted. The first 20 uniquely indexed powder line positions (overlapping positions removed) for the isostructural calcium–rare earth (R) borates, where R = La^{3+}, Nd^{3+}, Sm^{3+}, Gd^{3+}, Er^{3+}, and Y^{3+}, were used to estimate the unit cell parameters by least-squares methods. The obtained unit cell parameters are listed in Table IV. The obtained unit cell parameters correlate quite well with the ionic radii of the rare earth ions. The correlation coefficients between the unit cell lengths and the ionic radii[10] are all greater than 0.99 for the *a*, *b*, and *c* axes, respectively. The smallest relative increase in the cell parameters with the radii is observed for the *b* axis, followed by the *a* and *c* axes. The programs POWCAL and POWREF, used for calculating expected powder photographs from single-crystal X-ray intensity data, were written by one of us (R.N.).

Electron Microscopy Studies. *TEM Investigation.* Several crystals of the new $Ca_4SmO(BO_3)_3$ compound were ground in acetone and deposited on a holey carbon film supported on a copper grid. The crystals were identified by comparing their electron diffraction patterns (cf. Figure 2a) with the ones obtained by the X-ray diffraction studies, prior to any energy-dispersive X-ray analysis (EDX) and/or parallel electron energy loss spectroscopy (PEELS). The microscope used was a JEM-2000FX equipped with a Link AN 10000 EDX system and a Gatan M666 PEELS spectrometer. The PEELS spectra, recorded with an emission (LaB_6) current of 1 μA and a spectrometer entrance aperture of 1 mm, revealed edges (cf. Figure 1a,b) from the elements Sm, Ca, B, and O. The energy scale was calibrated against spectra recorded under identical conditions for NiO and BN crystals. Simultaneously recorded and computer evaluated[11] EDX spectra gave a charge balanced formula of $Ca_{3.9}Sm_{1.1}O(BO_3)_3$.

HTREM structure imaging was performed with a JEM-4000EX microscope operated at 400 kV and capable of a structural resolution of 0.16 nm. The structure image (cf. Figure 2) was compared with a computer simulated image (cf. Figure 2c) calculated with the coordinates of the atoms obtained by the X-ray diffraction study. The image calculations were performed with a local version of the SHRLI software package adopted for an IBM PS/2 computer. The parameters used in the calculations were;

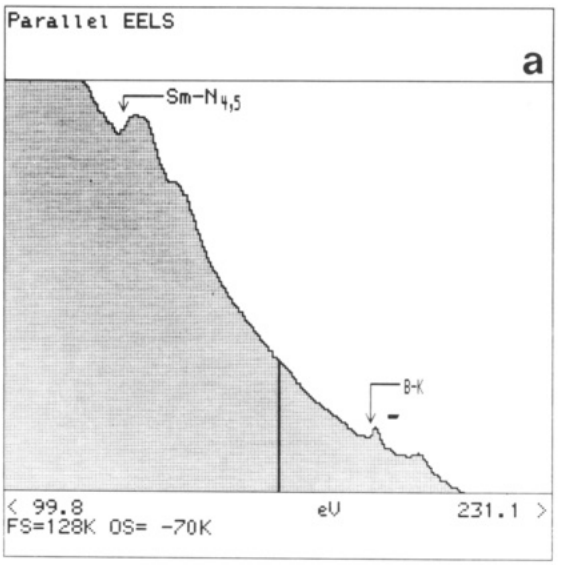

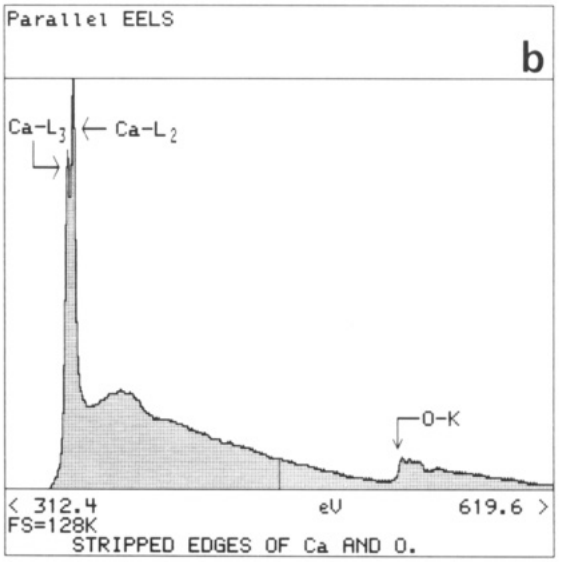

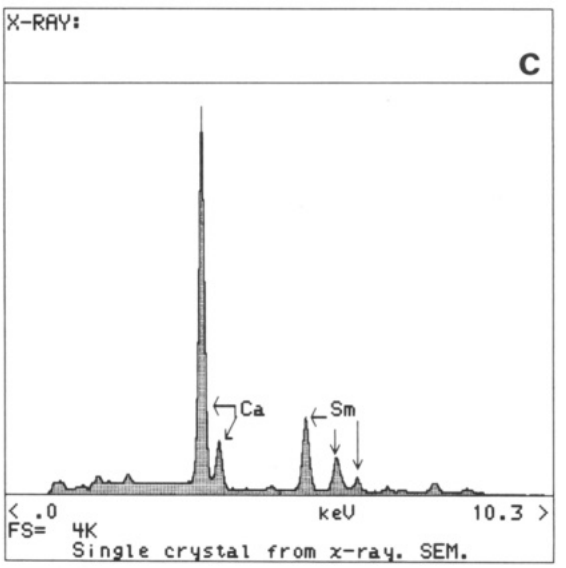

Figure 1. Electron energy loss spectra, EELS, recorded for a thin fragment of a synthesized $Ca_4SmO(BO_3)_3$ crystal, showing the EELS edges for (a) samarium and boron and (b) calcium and oxygen. (c) The energy-dispersive X-ray spectrum (EDX) from the $Ca_4SmO(BO_3)_3$ single crystal used for collecting the X-ray diffraction data.

(7) Sheldrick, G. M. SHELX-76. Program for crystal structure determination; University of Göttingen, 1976.
(8) *International Tables for X-Ray Crystallography*; Kynoch Press: Birmingham, 1974; Vol. IV.
(9) Dowty, E. ATOMS. A computer program for displaying atomic structures; Kingsport, 1989.
(10) Shannon, R. D. *Acta Crystallogr.* **1976**, *A32*, 751.
(11) Statham, P. J. *Microchim. Acta* **1979**, *8*, 229.
(12) Lei, S.; Huang, Q.; Zheng, Y.; Jiang, A.; Chen, C. *Acta Crystallogr.* **1989**, *C45*, 1861.
(13) Fletcher, J. G.; Glasser, F. P.; Howie, R. A. *Acta Crystallogr.* **1991**, *C47*, 12.

Table IV. Unit Cell Parameters (Å and deg) for the Synthesized Compounds, Isostructural to $Ca_4SmO(BO_3)_3$, Obtained from Least-Squares Fitting of Uniquely Indexed Line Positions on X-ray Guinier Powder Photographs[a]

composition	a	b	c	β	V, Å^3
$Ca_4LaO(BO_3)_3$	8.172 (1)	16.080 (2)	3.629 (1)	101.43 (2)	467.4 (2)
$Ca_4NdO(BO_3)_3$	8.131 (1)	16.056 (2)	3.593 (1)	101.38 (2)	459.8 (2)
$Ca_4SmO(BO_3)_3$	8.114 (1)	16.049 (2)	3.575 (1)	101.33 (2)	456.5 (2)
	[8.114 (2)]	[16.061 (4)]	[3.579 (1)]	[101.38 (3)]	[457.2 (2)]
$Ca_4GdO(BO_3)_3$	8.106 (2)	16.028 (3)	3.557 (1)	101.25 (2)	453.3 (3)
$Ca_4YO(BO_3)_3$	8.080 (2)	16.016 (3)	3.532 (1)	101.24 (2)	448.3 (2)
$Ca_4ErO(BO_3)_3$	8.075 (2)	16.008 (3)	3.530 (1)	101.18 (2)	447.6 (2)

[a] The parameters given within brackets for $Ca_4SmO(BO_3)_3$, included for comparison, were obtained from measurements on a single crystal diffractometer (cf. Table I) and are those used throughout the present study.

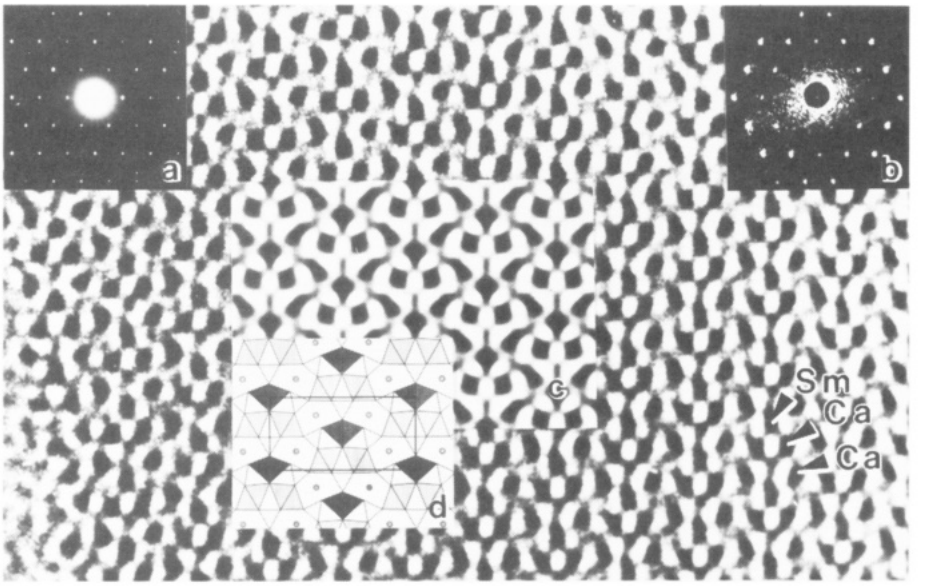

Figure 2. Structure image of $Ca_4SmO(BO_3)_3$ recorded with the electron beam parallel to [001]. The selected electron diffraction pattern (a) is inserted as well as an optical diffraction pattern (b) from approximately the area shown. A computer-simulated image (c) calculated from the structure and a polyhedral representation (d) of the structure (cf. Figure 4) is matched into the micrograph.

spherical aberration constant 1.0 mm, semiangle of beam convergence 0.25 mrad and half-width of spread of Gaussian focus 3.0 nm.

SEM Investigation. The $Ca_4SmO(BO_3)_3$ single crystal used for the X-ray diffraction study was demounted and analyzed in a scanning electron microscope (SEM), JSM-840A, equipped with a Link AN10000 EDX system. The EDX spectra (a typical one is shown in Figure 1c) were collected for many spots on the surface of the crystal. The evaluated spectra gave a charge balanced average formula for the crystal of $Ca_{3.90}Sm_{1.10}O(BO_3)_3$ in agreement with the previous EDX studies on other crystals from the specimen.

Discussion

A fragment of the structure of $Ca_4SmO(BO_3)_3$, showing the metal–oxygen bonds observed, together with the atomic labels used is shown in Figure 3. The location of the fragment in the unit cell is indicated in Figure 4, which shows one sheet of the oxygen coordination polyhedra in the structure, viewed along the short *c* axis. For clarity, the polyhedra around the Sm and Ca(2) atoms are drawn for the six nearest (<2.46 and <2.63 Å, respectively) oxygen atoms, thereby omitting the two longer bonds (>3.19 and >2.87 Å) that would make Sm and Ca(2) eight-coordinated. It should be noted that the octahedra drawn around Sm and Ca(2) become rather distorted. The octahedra around Ca(1) and Ca(2) are linked by edge sharing into walls that are two octahedra wide. The three-dimensional structure is formed by an infinite stacking of such sheets, due to edge sharing along **c** by the polyhedra around the Sm, Ca(1), and Ca(2) atoms.

A structure building unit can be considered to consist of five octahedra linked to three borate groups. The units are composed of one octahedron around a Sm atom, together with two pairs of octahedra related by mirror symmetry. Each such pair consists of the two octahedra around Ca(1) and Ca(2) that form a wall. The octahedra in the walls and those around the Sm atoms have one common corner (Figure 3), the O(1) atom. Except for this oxygen atom, all the other oxygens are borate oxygens. In the crystal, the structural units are linked together by corner-sharing and repeated by edge sharing in the **c** direction (cf. above) to give the composition $Ca_4SmO(BO_3)_3$. The structure is related to the recently determined structure of the calcium fluoroborate $Ca_5(BO_3)_3F$. The $Ca_4SmO(BO_3)_3$ and $Ca_5(BO_3)_3F$ structures are related (cf. Figure 5) to the common $Ca_5(PO_4)_3F$ fluorapatite structure.[14]

The Sm–O bond distance distribution is somewhat uneven. Two shorter Sm–O bonds of 2.25 and 2.27 Å are formed to the non-borate oxygen atoms O(1). These bonds extend parallel to the planes containing the **a** and **c** directions and explain why the *a* and *c* unit cell parameters increase more with increased ionic radii of the rare earth ion, than the *b* parameter (cf. above). The other four Sm–O bonds formed in the structure range 2.38–2.46 Å. Thus, the Sm atoms are located closer to one edge (formed by the O(1) atoms) of the distorted octahedra and the coordination can be considered to be of 2 + 4 type. As the Sm atom (and four of its coordinating oxygen atoms) is located in a mirror plane (e.g., $y = 0$) of the space group, the coordination around Sm has the point symmetry *m* (or

(14) Sudarsanan, K.; Mackie, P. E.; Young, R. A. *Mater. Res. Bull.* **1972**, *7*, 1331.

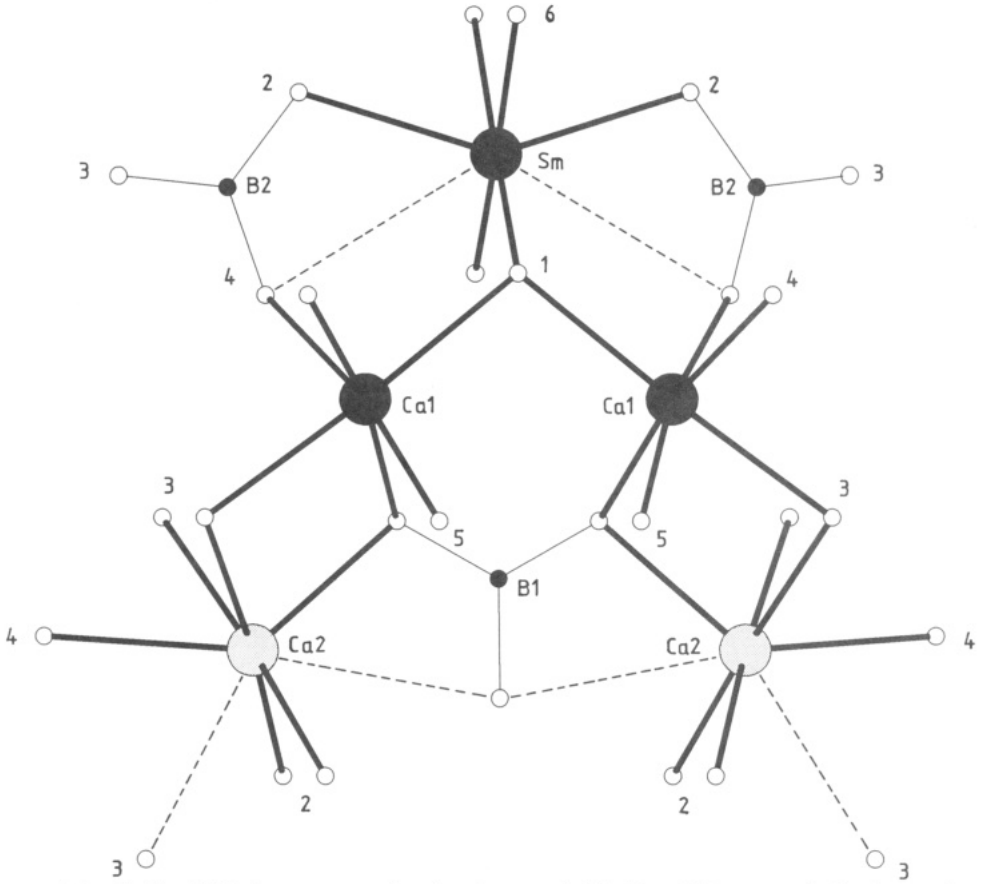

Figure 3. Fragment of the $Ca_4SmO(BO_3)_3$ structure, showing the atomic labeling of the atoms (only the numbers are given for the oxygens) and the metal–oxygen bonds. The projection direction is about 10° from [001]. The closely adjacent oxygen positions in the figure represent equivalent oxygen atoms related by one unit translation. The longer bonds (>2.8 Å) to Sm and Ca(2) are dashed. The location of the fragment in the unit cell is indicated in Figure 4.

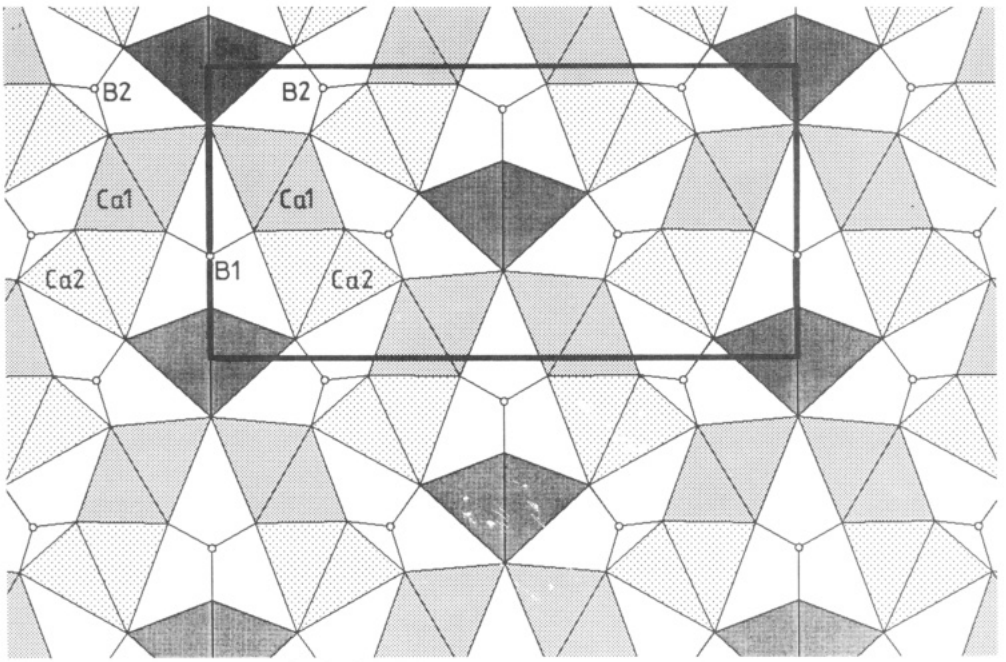

Figure 4. Polyhedral representation of the $Ca_4SmO(BO_3)_3$ structure, when projected along [001]. The polyhedra drawn around the Sm and Ca(2) atoms represent six-coordination. The metal positions labeled in the figure are those included in Figure 3. The origin of the unit cell is at the upper left corner, **b** is horizontal and the projection of **a** (on a^*) vertical.

C_s). The calculated centroid of the six coordinating oxygen atoms have the fractional coordinates (–0.0403,0,–0.0364) compared to the Sm position at (0,0,0). Thus, the Sm atom is displaced by 0.328 Å from the coordination centroid. Further away from the Sm atom there are two more Sm–O distances of 3.20 Å. If these two oxygens would be included into the description of the coordination around Sm, they can be considered as capping two adjacent faces of the distorted octahedra.

The oxygen octahedron around the calcium atom Ca(1) is more regular than that around the Sm atom, the six bond distances range from 2.33 to 2.39 Å. The coordina-

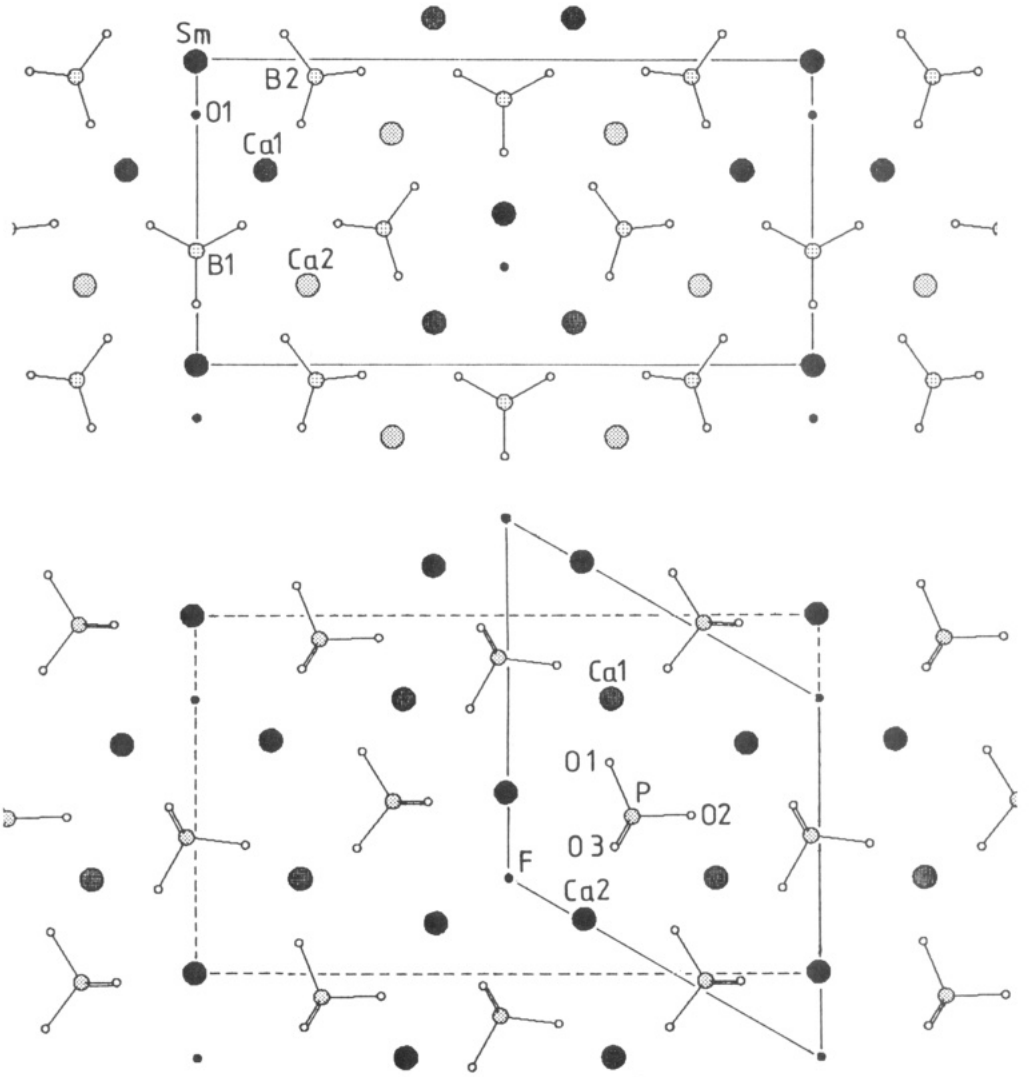

Figure 5. Projections of the $Ca_4SmO(BO_3)_3$ and the common fluorapatite $Ca_5(PO_4)_3F$ structures. For comparison, an area corresponding to the unit cell of $Ca_4SmO(BO_3)_3$ has been indicated by dashed lines in the fluorapatite structure.

tion around the Ca(2) atom can be considered to have a geometry similar to that of the Sm atom. Thus, the six shorter Ca(2)–O bonds range from 2.34 to 2.63 Å, and the coordination polyhedra can be considered as a distorted octahedron. Two longer Ca(2)–O bonds, from 2.87 to 2.96 Å, also occur, and the two oxygen atoms involved might be considered as capping two faces of the distorted octahedron. The borate groups are triangular, and the B–O bond distances of about 1.38 Å are in agreement with those found in other metal borates (Shannon[10] and, e.g., Norrestam et al.[15]).

As a simple comparison with known bond distance distributions in oxides, calculations of empirical bond valences with the present structural results have been performed, using the parameter values and the bond valence–bond distance correlation functions given by Brown and Altermatt.[16] As no parameter value is given for Sm^{3+}, a linear interpolation of ionic radii[9] vs determined bond valences for related ions (Eu^{3+} and Nd^{3+}) yield a reasonable estimate (r_0 = 2.083 Å) for the Sm^{3+} parameter. The bond valence sum, bvs, at the Sm^{3+} position becomes 2.83 when calculated for the six nearest oxygen neighbors and 2.93 if the two more distant O(4) oxygens are included, in rather close agreement with the expected value of 3.00. For the Ca(1) position the bvs is slightly higher (2.11) and for the Ca(2) position lower (1.91) than the expected 2.00 The bvs values at the boron positions B(1) and B(2) are close to 3.00, viz., 2.91 and 2.92. The values for the oxygen atoms range from 1.85 to 2.06. It could be noted that the two longest oxygen bvs values (1.85 and 1.90) are found for the oxygen atoms, O(3) and O(6), showing the largest thermal vibrations (cf. U_{eq} values in Table II). As all the estimated bvs values in general are in good agreement with the expected formal charges of the atoms, the bond distance distributions in the present structure investigation are rather normal and agree with the averaged distance distributions from which Brown and Altermatt[16] derived their parametrization.

The thermal parameters (U_{ij} in Table II) of the metal ions, show that the Sm and Ca(2) atoms vibrate rather anisotropically. The thermal ellipsoids of Sm and Ca(2) have, as indicated by their U_{ij} tensors, significant large components along the **b** direction. The vibrational anisotropy of Sm and Ca(2) agrees with the anisotropic shapes of their coordination polyhedra. The vibrations of the Ca(1) atom (and the shape of the coordination octahedron) are essentially isotropic.

It could be noted that the present structure type fulfills several of the requirements suggested[17] for possible high

(15) Norrestam, R.; Dahl, S.; Bovin, J.-O. *Z. Kristallogr.* **1988**, *187*, 201.
(16) Brown, I. D.; Altermatt, D. *Acta Crystallogr.* **1985**, *B41*, 244.
(17) Hong, H. Y.-P.; Chinn, S. R. *Mater. Res. Bull.* **1976**, *11*, 461.

Nd concentration laser materials. Thus, the $Ca_4NdO(BO_3)_3$ compound and/or Nd doped analogues (to obtain isolated $Nd-O_6$ coordination octahedra) with this structure type seem to be promising candidates for new minilaser materials. The structural features, including the fact that there is only one type of Nd position in the structure, make it possibly a better candidate than, e.g., the recently[3] suggested compound $Ba_3Nd_2(BO_3)_4$. Investigations along these lines but including also studies of the effects of including other alkaline earth ions are in progress.

Acknowledgment. We are indebted to Mr. A. Sjödin for his skillful assistance with the synthetic work. We also thank one of the referees for making us aware of the recent structural investigation of $Ca_5(BO_3)_3F$. The financial support of the Swedish Natural Science Research Council gratefully acknowledged.

Registry No. $Ca_4LaO(BO_3)_3$, 140656-50-4; $Ca_4NdO(BO_3)_3$, 140656-51-5; $Ca_4SmO(BO_3)_3$, 134775-92-1; $Ca_4GdO(BO_3)_3$, 140656-52-6; $Ca_4YO(BO_3)_3$, 140656-53-7; $Ca_4ErO(BO_3)_3$, 140656-54-8; $CaCO_3$, 471-34-1; B_2O_3, 1303-86-2; La_2O_3, 1312-81-8; Nd_2O_3, 1313-97-9; Sm_2O_3, 12060-58-1; Gd_2O_3, 12064-62-9; Er_2O_3, 12061-16-4; Y_2O_3, 1314-36-9.

Supplementary Material Available: Listings of observed and calculated structure factors (3). Ordering information is given on any current masthead page.

Additions and Corrections

1991, Volume 3.

Daniel J. Sandman, Rebecca A. Haaksma, and Bruce M. Foxman: Bis(*p*-chlorocinnamate) Ester of 2,4-Hexadiyne-1,6-diol: Crystallographic and Spectroscopic Studies of an Unreactive Crystal.

Page 475. In the course of studying the room-temperature solid-state emission spectra of polycrystalline samples of cinnamic acid and several of its derivatives, we observed the spectrum of *p*-chlorocinnamic acid (**3**) and found that it varied from our previous report. Accordingly, we reexamined the spectra of **2** and **3** using the same samples studied in our previous report, as well as freshly crystallized samples. For **2** and **3**, the maxima reported at 520 and 540 nm, respectively, are not observed. For **2**, the spectrum exhibits broad maxima near 370 and 395 nm; the excitation spectrum is as we previously reported. For **3**, the spectrum exhibits a broad maximum near 410 nm and includes the previously observed Raman-shifted line. The main feature of the excitation spectrum for **3** is a broad maximum near 370 nm. We thank Ms. E. A. Yost for technical assistance in the experiments.